Some aspects of uncertainty in predicting sea ice thinning

C. M. Bitz

Department of Atmospheric Sciences, University of Washington, Seattle, WA, USA

Abstract. A high proportion of the uncertainty in the decline of Arctic sea ice thickness in recent global climate models can be explained by the uncertainty in the ice thickness in the late 20th century. Experiments with one model indicate that this sensitivity to the mean state remains even when ice-albedo feedback is eliminated from the model. The magnitude of ice-albedo feedback is quantified and found to be too small to be a major source of uncertainty in thickness decline in climate models. Instead it is shown that the sea ice growth-thickness feedback in combination with large biases in the sea ice thickness during the 20th century can easily give rise to very large uncertainty in future thickness decline. Reducing biases in the surface fluxes and better tuning the surface albedo would improve uncertainty in both present and future prediction.

1. Introduction

Large and rapid changes in the Arctic sea ice in the past few decades have attracted attention to future sea ice predictions in global climate models. Models are consulted to see if future changes will continue at the current pace or if they will accelerate or decelerate [e.g., *Holland et al.*, 2006b]. But uncertainty (i.e., spread) in the 21st century sea ice predictions in the models used for the Intergovernmental Panel on Climate Change Fourth Assessment Report (IPCC AR4) is considerable [*Arzel et al.*, 2006; *Zhang and Walsh*, 2006]. Understanding the cause for this uncertainty could help scientists interpret the results of current models, and may help reduce the uncertainty in developing future models.

Some have claimed that a model's success at simulating the observed mean climatology and recent trends is a metric of model reliability for future forecasts [e.g., *Stroeve et al.*, 2007]. Indeed it has been shown that the mean state of sea ice strongly influences trends in the volume of Arctic sea ice in a given model. *Gregory et al.* [2002] found this to be true in a global climate model when they noted that sea ice volume declined more rapidly in the early 21st century simulation, when the sea ice was thicker and more extensive, and the rate of decline slowed long before the ice disappeared. The rate change could not be explained by a difference in forcing. This result may seem surprising if one expects that ice-albedo feedback increases as sea ice thins and therefore might cause sea ice decay to accelerate in the 21st century (e.g., see *Holland et al., 2006a* and counter arguments by *Winton, 2008*).

Bitz and Roe [2004] explained Gregory et al.'s results in terms of a strong negative feedback that depends inversely on sea ice thickness. When subject to an increase in downwelling longwave radiation, perennial sea ice melts faster during the melt season, but it also tends to grow faster in fall and winter. Faster winter growth causes the ice to rebound somewhat each winter. *Bitz and Roe* [2004] termed this negative feedback process the growth-thickness feedback. The growth rate is roughly inversely proportionate to thickness, such that thin ice rebounds far more than thick ice. Thus thicker ice will tend to thin much faster, and even if the forcing increases steadily, the rate of thinning slows down over time. Once perennial sea ice transitions to seasonal sea ice, the mechanism diminishes.

0148-0227/08/$9.00

Bitz and Roe [2004] did not account for the effect of positive ice-albedo feedback in their calculations. Here I expand upon the ideas of *Gregory et al.* [2002] and *Bitz and Roe* [2004] to investigate the role of the mean state on predicting uncertainty in sea ice retreat. In addition, I will quantify the influence of ice-albedo feedback in one model, and then estimate the role of uncertainty in ice-albedo feedback on uncertainty in predictions of sea ice retreat.

2. Thickness sensitivity in CMIP3 models

First I use the World Climate Research Programme's Coupled Model Intercomparison Project (CMIP3) to demonstrate that a high proportion of the uncertainty in the rate of Arctic sea ice thickness decline in models can be explained by the uncertainty in the ice thickness in the late 20th century. Plate 1a shows timeseries of annual mean sea ice thickness north of 70°N in the CMIP3 models (Table 1 lists the models). The thicker models thin at a much faster rate than the thinner models.

Trends from the early 21st century are plotted against the mean from the last half of the 20th century in Plate 1b. The corresponding correlation coefficient is R=-0.52 for all 19 models and R=-0.86 when models 5 and 10 are ignored. Sea ice retreat in model 5 becomes quite rapid beyond the time for which the trend was computed. The delay is probably due to ocean transients. A newer version of this model also appears in the CMIP3 archive (model 6), and it is in good agreement with the other models. I have no explanation for the unusual behavior in model 10.

The average ice thickness north of 70°N across the CMIP3 models is highly correlated with the September ice extent [R=0.80 for 1980-1999 averages according to Bitz et al., 2008]. Therefore understanding what controls the ice thickness and its uncertainty will also be informative for September ice extent. Presumably understanding uncertainty in wintertime ice extent would involve careful scrutiny of the ocean heat transport in models, which is not part of this study.

The remainder of the paper attempts to show in more detail how the mean state influences future thickness change and its uncertainty across models.In the next section, I quantify the effect of ice-albedo feedback in one model and show that the mean state strongly influences thickness change even when ice albedo is held fixed.

Table 1. The CMIP3 models used in this study.

Number	Modeling Center	Model Abbreviations
1	Bjerknes Centre for Climate Research (Norway)	BCCR BCM2.0
2,3	Canadian Centre for Climate Modelling and Analysis (Canada)	CCCMA CGCM3.1 T47, T63
4	Centre National de Recherches Meteorologiques, Meteo-France (France)	CNRM CM3
5,6	Commonwealth Scientific and Industrial Research Organization (Australia)	CSIRO MK3.0, MK3.5
7,8	Geophysical Fluid Dynamics Laboratory (USA)	GFDL CM2.0, CM2.1
9,10	Goddard Institute for Space Studies (USA)	GISS AOM, ER
11	Institute for Numerical Mathematics (Russia)	INMCM3.0
12,13	Center for Climate System Research (Japan)	MIROC3.2 MEDRES, HIRES
14	University of Bonn (Germany)	MIUB ECHO G
15	Max-Planck-Institut fuer Meteorologie (Germany)	MPI ECHAM5
16	Meteorological Research Institute (Japan)	MRI CGCM3.2.2A
17	National Center for Atmospheric Research (USA)	NCAR CCSM3
18,19	United Kingdom Meteorological Office (UK)	UKMO HADCM3, HADGEM1

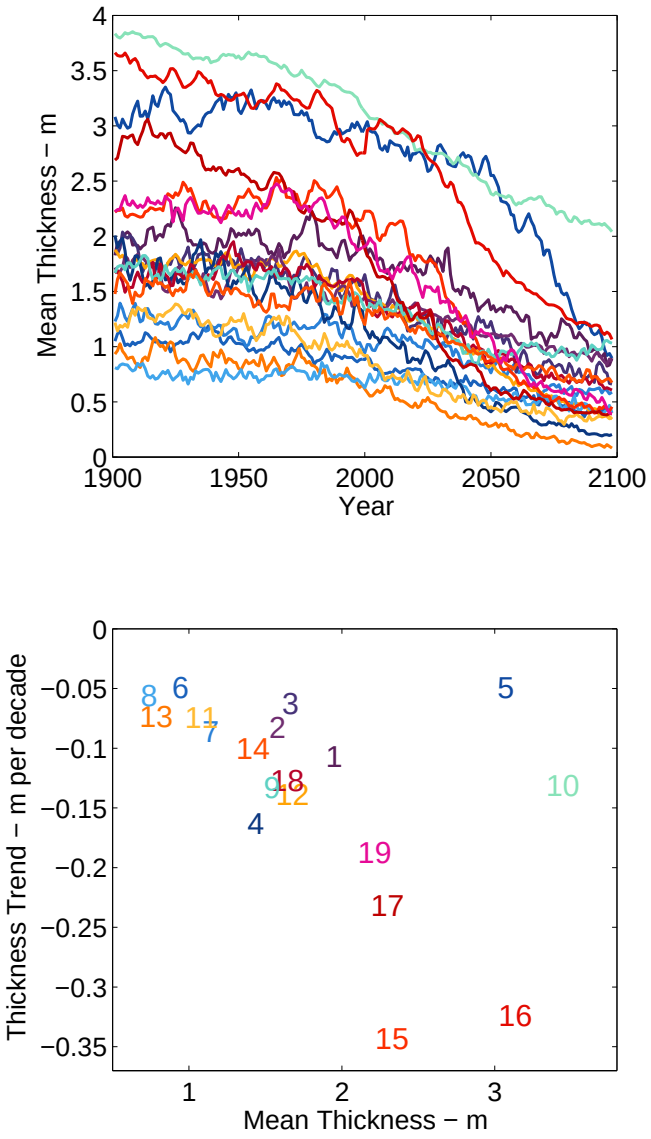

Plate 1. (a) Timeseries of mean ice thickness north of 70°N in CMIP3 models for the 20th century and SRES A1B future scenario. (b) Scatter plot of the thickness trend from 2010-2050 versus the mean from 1950-2000. The numbers corresponds to the order the models are listed in Table 1. The IAB FGOALS model was excluded because it has more than 10 m thick ice in the Arctic in the 20th century, and the IPSL CM4 model was excluded because the run archived at CMIP3 had an erroneous discontinuity in the aerosol forcing (Sébastien Denvil, pers. comm. 2008).

3. A measure of ice-albedo feedback

The Community Climate System Model version 3 (CCSM3) is used for a series of experiments to quantify the influence of ice-albedo feedback on sea ice thickness change in response to increasing carbon dioxide. CCSM3 has the third fastest rate of thinning among CMIP3 models in Plate 1. Hence, if ice-albedo feedback were the cause, one might anticipate that CCSM3 has above average ice-albedo feedback. This is advantageous because I intend to show that ice-albedo feedback is too small to cause much uncertainty in sea ice thickness change, even if it is uncertain within a factor of two.

3.1. Model Description

All components of CCSM3 in the experiments are standard, except the ocean is a slab mixed-layer, rather than the full ocean general circulation model, so the model can be run to equilibrium in only a few decades. The slab ocean has depth that is variable in space, but fixed in time, and the ocean heat transport is prescribed from a climatological monthly-mean annual cycle that was derived from a long control run of CCSM3 with the standard ocean component.

The slab ocean and sea ice share a horizontal grid with 320 x 384 points, with resolution varying 0.5-1°in the polar regions. The Northern Hemisphere pole of this grid is displaced to a point within Greenland. The atmosphere and land model's horizontal resolution is truncated spectrally at T42 and there are 26 vertical levels in the atmosphere.

The sea ice component in the experiments is distinct from the very simple motionless sea ice component that is part of the often used slab ocean option in the atmosphere component of CCSM. Here, the sea ice model resolves a distribution of ice thicknesses using multiple ice categories, each having a unique and variable concentration and thickness of ice and snow and a unique surface energy balance, surface albedo, and vertical temperature profile [*Bitz et al.*, 2001; *Lipscomb*, 2001]. The surface albedo is parameterized as a function of snow depth, sea ice thickness, and surface temperature. Melt ponds are not explicitly modeled, but their influence is parameterized crudely by the dependence of the albedo on temperature. The model momentum equation includes the elastic-viscous-plastic stress tensor of *Hunke and Dukowicz* [2002]. The model also employs an explicit brine pocket parameterization with shortwave radiative transfer through the ice from *Bitz and Lipscomb* [1999]. The inclusion of ice dynamics, multi-layer thermodynamics, and an ice-thickness distribution have been shown to affect the climate in coupled models [*Bitz et al.*, 2001; *Holland et al.*, 2001, 2006a]. The polar climate of the 20th and 21st century in this model is discussed in *Meehl et al.* [2006] and *Holland et al.* [2006a]. The other components of CCSM3 and its climatology are described in greater detail in *Collins et al.* [2006].

Table 2. Experiments conducted with CCSM3 in this study

Experiment name	CO_2	Description
Normal Control	355 ppm	Control integration with freely varying albedo
Fixed-Albedo Control	355 ppm	Sea ice and ocean albedo fixed to a climatology from the normal control
Normal Perturbed	710 ppm	CO_2 raised to represent mid-century anthropogenic forcing
Fixed-Albedo Perturbed	710 ppm	CO_2 raised with sea ice and ocean albedo fixed to a climatology from the normal control

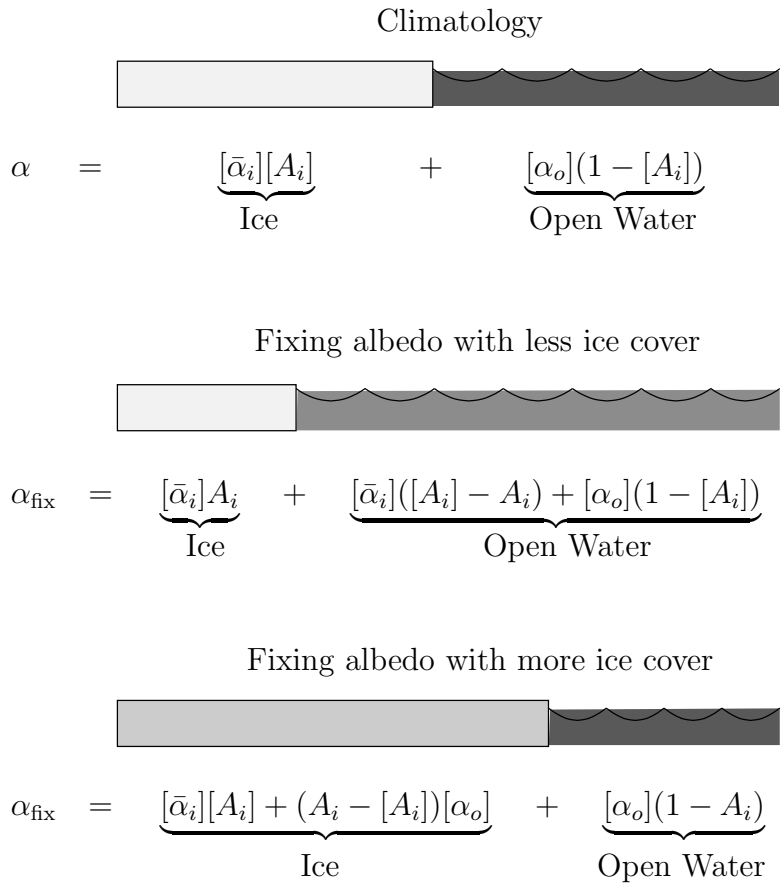

Figure 1. Illustration of how the grid cell average albedo is fixed in a run with evolving ice fraction. The shading of the ice and ocean in the illustration is meant to crudely indicate the relative reflectivity. If the ice covered portion of a grid cell in a run with the albedo fixed should fall below (rise above) the climatological ice fraction, the albedo of the open water (ice covered) portion is increased (decreased) to compensate. For simplicity, the ice-thickness distribution is represented by a single rectangle to indicate the total ice-covered fraction of the grid cell.

3.2. Experiments

To evaluate the effect of sea ice-albedo feedback on climate, pairs of experiments were run with the surface albedo allowed to vary and with it held fixed over sea ice, and ocean and the sensitivity to doubling CO_2 was evaluated. First a normal control integration was run with 1990s greenhouse gas concentrations (CO_2 at 355 ppm). Then a second control was run but with the surface albedo held fixed to a climatological monthly-mean annual cycle that was computed from the normal control. This new "fixed-albedo control" also had 1990s greenhouse gas concentrations. It was used to verify that the method of fixing the albedo achieves a very similar climate to the normal control. Finally, a pair of perturbed CO_2 experiments was run with CO_2 at 710 ppm: One with the albedo free to vary and a second with the surface albedo held fixed to the climatology from the normal control. Doubling CO_2 is representative of the anthropogenic forcing level at about mid-century in the SRES A1B scenario. In all four runs, the ocean heat transport is the same. Table 2 summarizes this quartet of runs.

The surface albedo in CCSM3 is decomposed into two spectral bands, denoted visible and infrared, for wavelengths above and below 700nm. These two bands are further decomposed into direct and indirect beam components. For simplicity I will describe the method for fixing the albedo as if there were only a single component, but in practice this method is applied to each of the four components separately. Because the weighting of the four components depends on clouds and atmospheric composition, which I am not fixing, the total surface albedo in the grid cell may still vary slightly.

The grid-cell average albedo (for each albedo component) is the weighted sum of the albedo for the sea ice covered fraction and the open water fraction:

$$\alpha = \bar{\alpha}_i A_i + \alpha_o (1 - A_i), \tag{1}$$

where $\bar{\alpha}_i$ is the albedo averaged over all ice-thickness categories, α_o is the albedo of open water, and A_i is the fraction

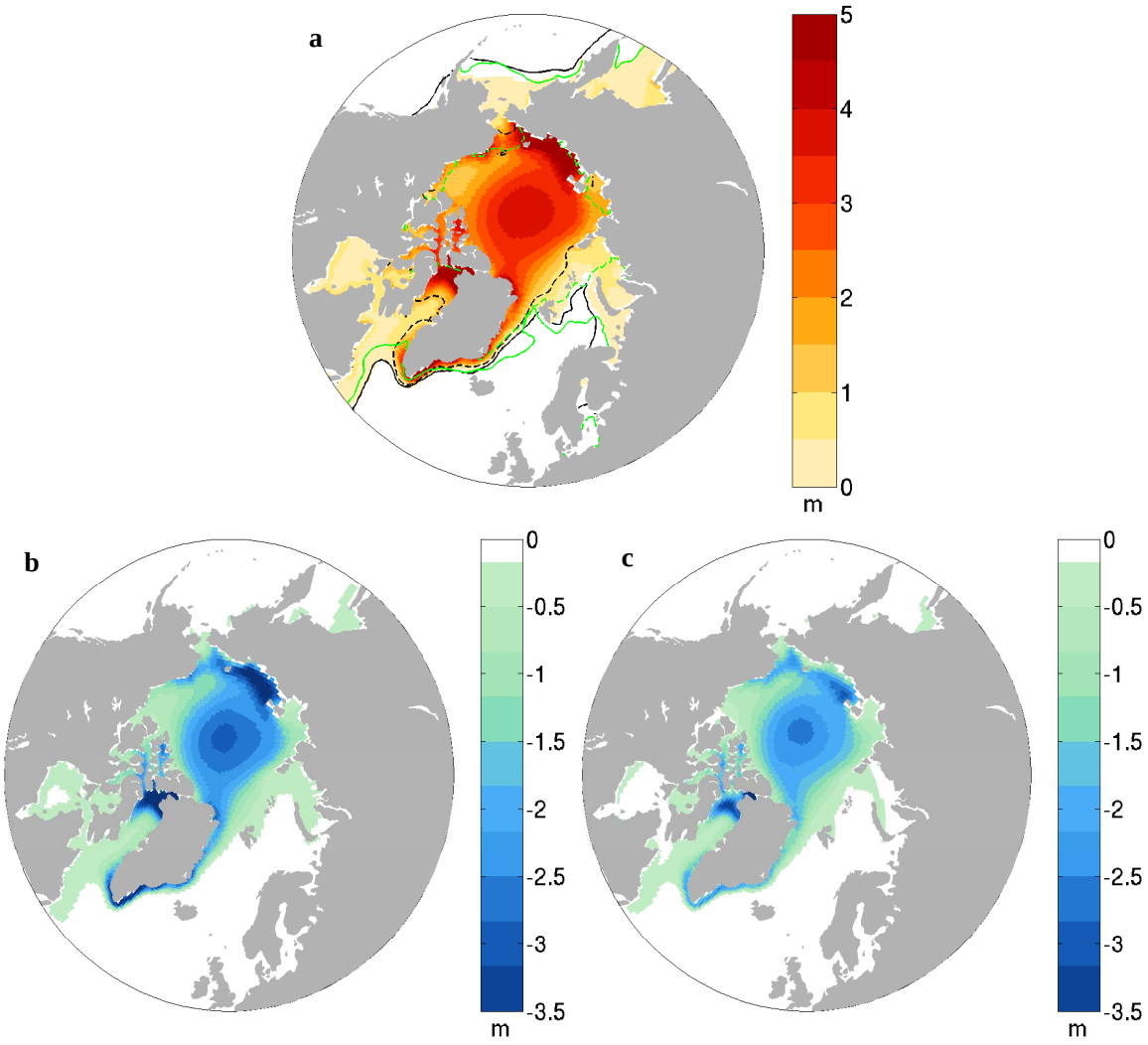

Plate 2. (a) Annual mean sea ice thickness in the normal control with contour of 15% ice concentration for March (solid) and September (dashed) for the control (black) and 1979-2000 passive microwave (green) [*Comiso*, 1995]. (b) Annual mean thickness difference between perturbed and control. (c) Annual mean thickness difference between fixed-albedo perturbed and control.

of the grid cell covered by sea ice. In the fixed-albedo runs, the grid-cell average albedo is fixed to

$$\alpha_{\rm fix} = [\bar{\alpha}_i][A_i] + [\alpha_o](1 - [A_i]), \qquad (2)$$

where the brackets denote the climatological monthly-mean annual cycle that is taken from the normal control run.

Even though the grid-cell average albedo is held fixed, the ice fraction may depart from the climatological mean according to the evolution of the climate in the model (particularly when CO_2 is raised to 710 ppm). When this occurs, $\bar{\alpha}_i$ or α_o is adjusted to maintain $\alpha = \alpha_{\rm fix}$, as illustrated in Fig. 1.

The sea ice thickness in the model exhibits considerable low frequency variability. As previously discussed by *Bitz et al.* [1996], the variability is a strong function of the mean thickness, such that thicker ice is far more variable (see Fig. 2). Therefore the control runs are at least 150 years long and all averages were taken for the last 100 years. The perturbed runs, which are thinner, were run for at least 80 years and averages were taken for the last 50 years (thinner ice also equilibrates faster, see Bitz and Roe, 2004).

The procedure for fixing the albedo succeeded to the extent that the fixed-albedo control reproduces the total surface albedo (sum of all four components) of the normal control when averaged June-August with an average random error of 0.0095 (the standard deviation across grid cells with sea ice) and a systematic error of 0.006 (the average difference across grid cells with sea ice). The average total surface albedo over the same area and months is 0.5. Hence compared to the total, the random error is less than 2% and the systematic error is about 1.2%. When comparing the total surface albedo in the fixed-albedo perturbed run to the fixed-albedo control, the errors are even lower, with a random error of 0.2% and a systematic error of 0.7%.

The sea ice thickness in the fixed-albedo control has nearly the same pattern of thickness in the normal control, but it tends to be 10-30 cm thicker in the Arctic Ocean (see Fig. 2, with an across grid-cell average random error of 33 cm and systematic error of 19 cm in 100-yr averages from each control. This thickness difference is almost 10% of the model's mean ice thickness in the Arctic Ocean. Because the percentage of systematic error in the surface albedo is so much smaller, it would appear that variations in the surface albedo have a nonlinear influence on sea ice thickness.

The goal of this study is to investigate the influence of the mean thickness on the 21st century sea ice retreat. The difference in the mean state of the fixed-albedo control and

the normal control is therefore an issue that must be considered. In the next section, changes from doubling CO_2 are computed with respect to the control that corresponds to the experiment: Normal perturbed is compared to normal control and fixed-albedo perturbed is compared to fixed-albedo control.

3.3. Ice-albedo feedback quantified

The annual mean ice thickness and March and September extents from the normal control are shown in Plate 2a. As in many climate models [see e.g., *Holland and Bitz*, 2003], the thickness pattern is biased. The thickest ice appears in the Chukchi Sea and in the center of the Arctic Ocean, rather than next to the Canadian Archipelago. These biases result primarily from errors in the surface circulation in the model [*Bitz et al.*, 2001]. The thickness biases in CCSM3 are significantly reduced in integrations at T85 [*DeWeaver and Bitz*, 2006]. Thus the ice thickness patterns in CCSM3 runs in CMIP3, which used T85 resolution, are much better. In addition the transient forcing during the 20th century leads to a somewhat thinner Arctic by the end of the 20th century compared to the fixed forcing 1990s control. In spite of the biases in Plate 2a, the experiments are nonetheless useful for evaluating general relationships among ice-albedo feedback, the mean state, and the response to anthropogenic forcing.

The change in sea ice thickness that results from doubling CO_2 with freely varying albedo is shown in Plate 2b, and the change with fixed albedo is shown in Plate 2c. It is clear that the pattern of thickness change is a strong function of the control thickness. As in the across-model analysis with the CMIP3 models, the thickness changes most where ice is thickest in the control. Although the overall magnitude of change is less without ice-albedo feedback, the functional dependence on the control thickness appears broadly the same.

The influence of ice-albedo feedback can be made more explicit by dividing the two thickness change maps in Plate 2b and c, as shown in Plate 3a. In the parlance of feedback analysis from electrical engineering, this quantity is called the "gain":

$$G = \Delta h / \Delta h_0, \tag{3}$$

where Δh is the thickness change in the normal perturbed case and Δh_o is the thickness change from the same perturbation but in the absence of some feedback (or feedbacks), which here is the ice-albedo feedback. Δh_o can also be thought of as the thickness change of a "reference system" [*Roe and Baker*, 2007], which comprises all the feedbacks in the system except the feedback that gives rise to the gain.

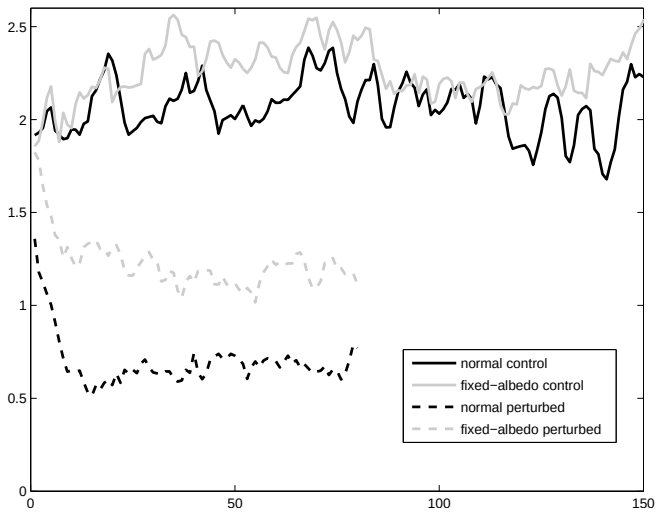

Figure 2. Timeseries of mean ice thickness north of 70°N in CCSM3 experiments (see Table 2).

The gain from ice-albedo feedback ranges from about 1.1 to 1.5 in most of the Arctic, with an average of 1.26 north of 70°N. The gain tends to be larger near the location of the ice edge in summer, at the interface of the perennial and seasonal ice. The gain also appears somewhat noisy in spite of the long time periods that were used to compute the means.

A feedback factor f can also be defined such that

$$\Delta h = \frac{\Delta h_o}{1-f}, \tag{4}$$

where f is related to G by $f = 1 - G^{-1}$. Plate 3b shows f for CCSM3. Where $G > 1$, the feedback factor is positive, which is the case for all but a few tiny areas. In most of the Arctic, f varies between about 0.1 and 0.3, with an average of 0.21 north of 70°N. The error in my estimate of f that results from variability in the mean thickness north of 70°N is 0.02. The closer f is to one, the closer the system is to experiencing a runaway feedback. Although f indicates ice-albedo feedback is positive, it is not very big.

4. Influence of ice-albedo feedback on uncertainty in future thickness

In a recent landmark paper, *Roe and Baker* [2007] showed that much of the uncertainty in climate model predictions of future global mean warming could be estimated analytically from the uncertainty in climate feedbacks. I shall borrow heavily from their work to show that, in contrast, uncertainty in ice-albedo feedback has very little influence on the uncertainty of 21st century ice thickness trends among CMIP3 models.

In the equation of climate sensitivity for global temperature change (ΔT):

$$\Delta T = \frac{\Delta T_o}{1-f}, \tag{5}$$

ΔT_o derives from assuming a blackbody planet, in which blackbody radiation emitted by the planet stabilizes the climate by cooling (or warming) the planet when the planet exceeds (or falls below) its equilibrium temperature and f is the feedback factor (this time for ΔT, not Δh). Thus the most basic negative feedback process for stabilizing temperature is normally excluded from f, and instead its influence is contained in the reference climate sensitivity ΔT_o. For the blackbody planet assumption, ΔT_o can be estimated from the first term in a Taylor's series expansion:

$$\Delta T_o = \left[\frac{\partial}{\partial T}\sigma T^4\right]^{-1}_{T_E} \Delta R, \tag{6}$$

where σT^4 is the Steffan-Boltzmann law, T_E is the effective radiative temperature of the planet, and $\Delta R \approx 3.2 \mathrm{Wm}^{-2}$ is an estimate of the change in the top of atmosphere outgoing longwave radiation when CO_2 is doubled. Because σT^4 is well approximated by a tangent line, the first term in the Taylor's series is a good approximation. In other words, the temperature dependence of ΔT_o is easily neglected and Eq. 6 gives $\Delta T_o = 1.2$ °C, which is fairly accurate for a wide range of temperatures.

Roe and Baker [2007] note that f in Eq. 5 is on average about 0.65 for recent climate models. Hence the feedback factor that affects global temperature change is about three times larger than the one I estimated for the influence of ice-albedo feedback on sea ice thickness.

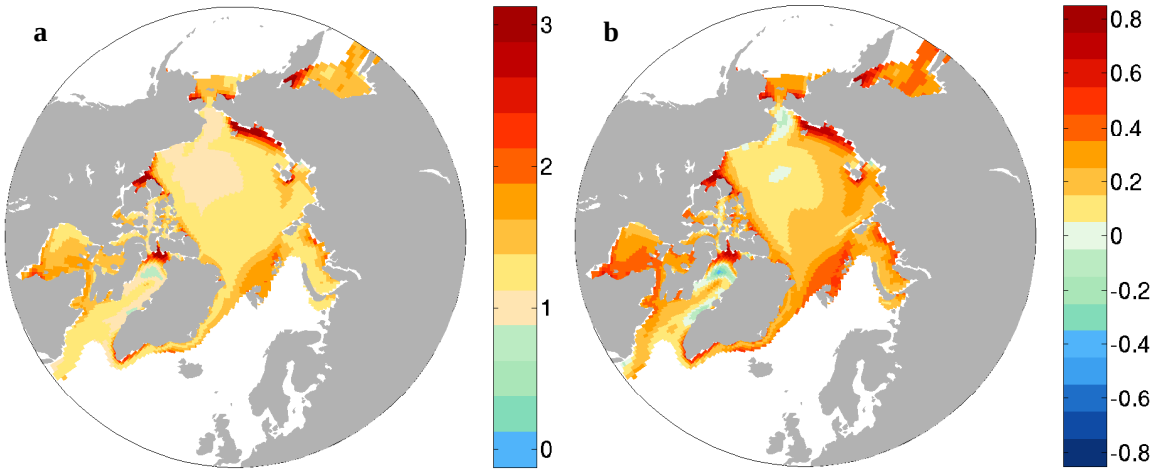

Plate 3. (a) Gain to ice thickness from ice-albedo feedback, computed from the ratio of Δh (Plate 2b) to Δh_o (Plate 2c). (b) Feedback factor on ice thickness from ice albedo feedback.

A number of studies have attempted to estimate what portion of f in Eq. 5 results from the influence of ice-albedo feedback on global mean temperature — not to be confused with the influence of ice-albedo feedback on sea ice thickness. *Bony et al.* [2006] summarize estimates of ice-albedo feedback in three studies and find a mean ice-albedo feedback factor of about 0.12 with a range of about -0.03 to .4. (Note that I have used a different definition for feedback than Bony et al, so I have had to convert their estimates to match my definition.) For reference from CCSM3, I find the feedback factor on global mean temperature for all feedbacks is 0.57 and for ice-albedo feedback alone it is 0.24. (There is no reason to expect that ice-abledo feedback should have the same feedback factor for global mean temperature as it does for ice thickness.)

Roe and Baker [2007] also pointed out that it is possible to compute the uncertainty in ΔT that results from uncertainty in f. Specifically, the uncertainty can be related to the probability density function $D_T(\Delta T)$ that the global temperature change is ΔT. And the distribution in ΔT can be related to a distribution in f by

$$D_T(\Delta T) = D_f(f)\frac{df}{d\Delta T}. \tag{7}$$

Roe and Baker [2007] assumed a normal distribution for f, with mean $\bar{f}$ and variance σ_f^2,

$$D_f(f) = \frac{1}{\sqrt{2\pi}\sigma_f}\exp\left[-\frac{(f-\bar{f})^2}{2\sigma_f^2}\right], \tag{8}$$

and then computed the resulting distribution for ΔT,

$$D_T(\Delta T) = \frac{1}{\sqrt{2\pi}\sigma_f}\frac{\Delta T_o}{\Delta T^2}\exp\left[-\frac{(1-\bar{f}-\Delta T_o/\Delta T)^2}{2\sigma_f^2}\right] \tag{9}$$

With the same basic relation between ice thickness and feedback as with global mean temperature and feedback, by analogy the distribution for Δh is

$$D_h(\Delta h) = \frac{1}{\sqrt{2\pi}\sigma_h}\frac{\Delta h_o}{\Delta h^2}\exp\left[-\frac{(1-\bar{f}-\Delta h_o/\Delta h)^2}{2\sigma_f^2}\right] \tag{10}$$

Here, I use this equation to represent the distribution of the thickness change averaged north of 70°N owing to ice-albedo feedback, so all variables in Eq. 10 are considered averaged north of 70°N as well.

Figure 3 shows examples of distributions from Eqs. 9 and 10 that arise from doubling CO_2. The parameters used for the distribution of ΔT ($\Delta T_o = 1.2$°C, $\bar{f} = 0.65$, and $\sigma_f = 0.13$) are derived from recent climate models as discussed in *Roe and Baker* [2007]. The parameters used for the distributions of Δh are $\bar{f} = 0.21$, estimated from CCSM3 (see section 3.3); $\Delta h_o = -1$ m, chosen to give a peak in the distributions at a little over one meter; and $\sigma_f = 0.1$ for the narrowest and $\sigma_f = 0.21$ for the slightly broader distribution.

I do not know the correct values for $\bar{f}$ and σ_f that represent the mean and uncertainty of the influence of ice-albedo feedback on ice thickness from current models. My estimate of uncertainty in f from just one model is bound to be much smaller than the range of f across models. Presumably the main factors that give rise to different values of f across models are difference between open ocean and sea ice albedos and how the ocean-ice heat flux is partitioned between lateral and basal melt. However, Fig. 3 shows that even a very large σ_f gives a narrow distribution for Δh. With an uncertainty of 100% of $\bar{f}$ (σ_f=0.21), ice-albedo feedback still only has a rather modest influence on uncertainty in Δh because f is so small. In contrast, the feedbacks that influence global mean temperature give an f that is more

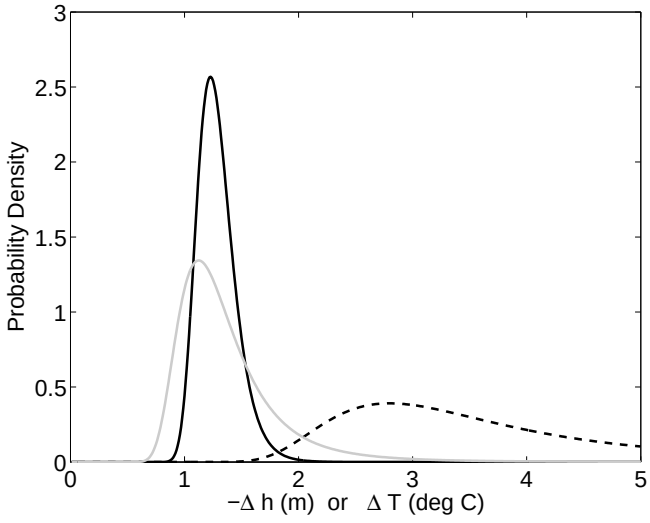

Figure 3. Distributions from Eqs. 9 and 10 for Δh (with $\Delta h_o = -1$ m, $\bar{f} = 0.21$, and $\sigma_f = 0.1$ for the black line and $\sigma_f = 0.21$ for the grey line) and ΔT (dashed line, with $\Delta T_o = 1.2$°C, $\bar{f} = 0.65$, and $\sigma_f = 0.13$). The distributions for Δh are much narrower because $\bar{f}$ is much smaller for h than for T.

than three times larger. Even a small uncertainty in f is important as f approaches 1 because $1-f$ appears in the denominator of Eqs. 4 and 5. Thus a more important issue is whether I have underestimated $\bar{f}$. I have let $\bar{f}=0.21$, which is the feedback factor I computed for CCSM3 in the previous section. This is unlikely to be an underestimate of the true $\bar{f}$ for the CMIP3 models because CCSM3 has among the highest Arctic climate sensitivity of any CMIP3 model [*Bitz et al.*, 2008].

5. The influence of the mean state on uncertainty in future thickness

Because the present-day thickness north of 70°N in the CMIP3 model differs by more than a factor of 3 (see Fig. 1), an estimate of the uncertainty caused by errors in the mean state is in order. Sea ice is stabilized primarily by the inverse relation between net sea ice growth and thickness, which *Bitz and Roe* [2004] called the growth-thickness feedback process. On an annual mean basis and provided the climate conditions are not too anomalous, sea ice experiences net melt (growth) when the ice exceeds (falls below) its equilibrium thickness. This leads to an adjustment process, which was described by *Untersteiner* [1961] and *Untersteiner* [1964], that yields an equilibrium thickness. The growth adjustment can be considered analogous to the blackbody-radiative adjustment process that causes the planet to reach an equilibrium temperature.

When the climate is perturbed, such as by increasing CO_2, this adjustment process acts to damp the response somewhat. However, for sea ice, the damping is a strong function of thickness itself. In other words, Δh_o is a strong function of h, while as explained above ΔT_o is nearly a constant. *Bitz and Roe* [2004] calculated the dependence of Δh_o on h for an idealized coupled atmosphere and ice slab without ice-albedo feedback using the formulation in *Thorndike* [1992]:

$$\widehat{\Delta h_o} = -\frac{(kn_w+Bh)^2}{Bn_wk(-A/n_w+D/2)}\left[-\frac{1}{n_w}-\frac{1}{n_s}+\frac{hB/n_w}{kn_w+Bh}\right]\Delta A, \tag{11}$$

where the parameters and variables are defined in table 3. The hat over Δh_o is added to emphasize that this idealized model lacks many processes that I had lumped into Δh_o above. The term in brackets in Eq. 11 has a fairly weak thickness dependence, so its h can be replaced with a constant $\bar{h}$ and the leading dependence on h is parabolic:

$$\widehat{\Delta h_o} \approx -(q+rh)^2, \tag{12}$$

where q and r are independent of h.

Bitz and Roe [2004] considered how ice export might alter Eq. 12. *Hibler and Hutchings* [2002] (updated in *Hibler et al.*, 2006), argue that export increases with thickness for ice thickness between about 0 and 4 m. *Bitz and Roe* [2004] reasoned that this sensitivity of export on the mean state is likely to enhance the sensitivity of Δh_o to h among models with ice in motion, which is the case for nearly all CMIP3 models. Neglecting the influence of the mean state on export here gives a conservative estimate for the the uncertainty in thickness change due to uncertainty in the mean state.

Given a distribution for h, $D_h(h)$, the distribution of $\widehat{\Delta h_o}$ is

$$D_{h_o}(\widehat{\Delta h_o}) = D_h(h)\frac{dh}{d\widehat{\Delta h_o}}. \tag{13}$$

If h is assumed to be normally distributed with mean $\bar{h}$ and variance σ_h^2, then using Eq. 12 and Eq. 8 with f replaced by h gives

Table 3. Definitions for the idealized analytic model

	Variables	
h	Annual mean ice thickness	variable
$\widehat{\Delta h_o}$	Thickness change for idealized model	variable
ΔA	radiative forcing	22.6 Wm^{-2}
A	σT_f^4 with T_f=273K	320Wm^{-2}
B	$4\sigma T_f^3$	4.6Wm^{-2}
k	Thermal conductivity	2 $\mathrm{Wm}^{-1}\mathrm{K}^{-1}$
$n_{w,s}$	Optical depth for winter or summer	2.5 or 3.25
D	Atmospheric heat transport	100Wm^{-2}

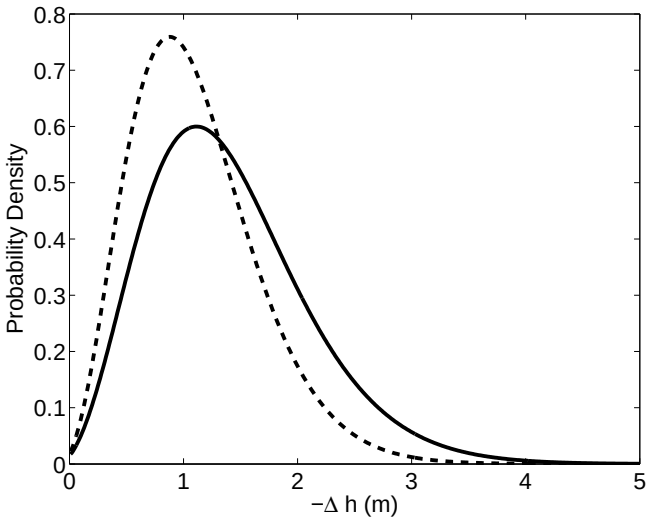

Figure 4. Distributions from Eqs. 14 and 15 for Δh_o (dashed line) and Δh (solid line) with $\bar{h}=1.8$ m, $\sigma_h=0.77$ m, $f=0.21$, and $\sigma_f=0$.

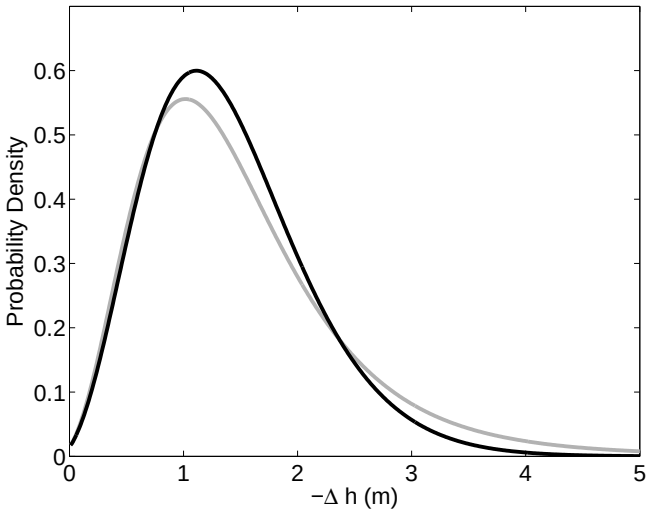

Figure 5. Distributions from Eq. 16 for Δh with $\sigma_f=0.21$ (grey line) and with $\sigma_f=0$ (black line, which is identical to the black line in Fig. 4). Both lines have $\bar{h}=1.8$ m, $\sigma_h=0.77$ m, and $f=0.21$.

$$D_{h_o}(\widehat{\Delta h_o}) \approx \frac{1}{2r\sigma_h\sqrt{-2\pi\widehat{\Delta h_o}}} \exp\left[-\frac{\left[\left(\sqrt{-\widehat{\Delta h_o}}-q\right)/r-\bar{h}\right]^2}{2\sigma_h^2}\right] \quad (14)$$

Now if $\widehat{\Delta h_o}$ is the only source of uncertainty in Δh, then

$$D_h(\Delta h) = D_{h_o}(\widehat{\Delta h_o})\frac{d\widehat{\Delta h_o}}{d\Delta h} = D_{h_o}(\Delta h(1-f))(1-f) \quad (15)$$

Figure 4 shows examples of distributions from Eqs. 14 and 15 that arise from doubling CO_2, but without any uncertainty in f (hence $\sigma_f = 0$). Again I use these equation to represent the distribution of thickness change averaged north of 70°N, so I have taken averages north of 70°N that give $\bar{h} = 1.8$ m and $\sigma_h = 0.77$ m from the CMIP3 models for 1950-2000 (see Fig. 1) and $f = 0.21$ from CCSM3 (see section 3.3). The distribution for Δh is influenced by ice-albedo feedback such that it is broader and the thickness change is larger than for Δh_o.

It is possible to compute the distribution of Δh with uncertainty in both Δh_o (via h) and f by computing the ratio of distributions. The result is the Mellin convolution

$$D_h(\Delta h) = \int_{-\infty}^{1} D_f(f) D_{h_o}(\Delta h(1-f))(1-f)df \quad (16)$$

[see, e.g., *Springer*, 1979]. A numerical solution to this integral is shown in Fig. 5 with the same parameters as in the previous paragraph except $\sigma_f = 0.21$. Uncertainty in f increases slightly the probability of greater thickness change at the expense of decreasing the probability of the peak.

6. Discussion

I have estimated the uncertainty from two primary thermodynamic feedbacks: Ice-albedo feedback and the growth-thickness feedback. No doubt there are also feedbacks between the ice and ocean that vary from model to model and these feedbacks may also depend on the mean state. Because I have not accounted for them, I have focused on ice thickness north of 70°N, where I expect far less influence from the ocean than in the subpolar seas. I have also not tried to quantify the uncertainty in how models treat sea ice dynamics and ice export. My estimates of the distribution widths should be thought of as a lower limit.

For simplicity (and by analogy to the work of *Roe and Baker* [2007]) the distributions here are meant to represent the climate in equilibrium after doubling CO_2. In the future scenario shown in Fig. 1, the trends of sea ice thinning in the early 21st century span almost an order of magnitude. I have assumed that the uncertainty in equilibrium ice thickness change from doubling CO_2 would be similar.

Earlier I noted that the CMIP3 models with thicker ice in the late 20th century thin at a faster rate in the early 21st century (see Plate 1a). As a result the uncertainty in mean ice thickness among CMIP3 models tends to decline in time over the two centuries. Figure 6 recasts estimates of the probability density functions from the previous section in terms of thickness rather than thickness change to illustrate this narrowing of uncertainty in time. The distribution in thickness becomes more sharply peaked after doubling CO_2, especially when the gain from ice-albedo feedback is included.

In the experiments described here, CO_2 was increased from 355 to 710 ppm, so the albedo effect is evaluated for a perturbation that transforms most of the perennial ice to seasonal ice in the Arctic Ocean in CCSM3. This forcing is roughly equivalent to the total anthropogenic forcing in the first half of the 21st century of the SRES A1B scenario. Experiments were run with CO_2 raised to just 550 ppm as well (not shown), which gave nearly the same estimate for the ice albedo feedback factor on ice thickness f in CCSM3. Because f depends little on the magnitude of the perturbation, I expect f would not vary much during a transient integration either.

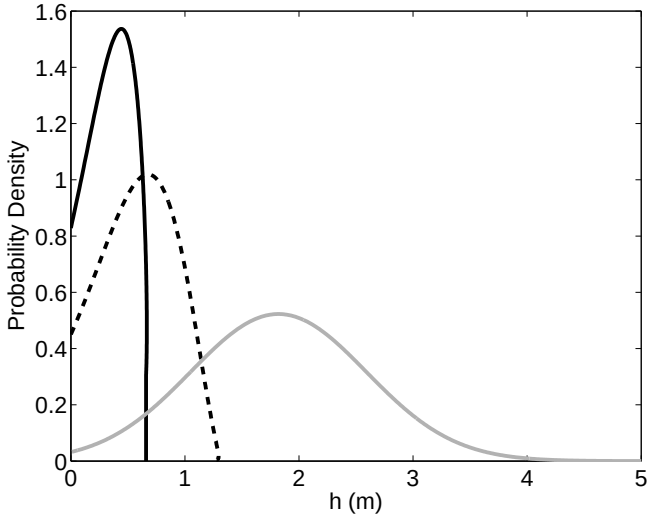

Figure 6. Distributions recast as a function of ice thickness rather than change in ice thickness, showing that the distribution narrows as the ice thins. The grey line is the initial assumption of a normal distribution of ice thickness with $\bar{h} = 1.8$ m and $\sigma_h = 0.77$ m. The other two lines are distributions after doubling CO_2 without ice-albedo feedback ($f = 0$, dashed line) and with ice-albedo feedback ($f = 0.21$ and $\sigma_f = 0$, black line).

7. Conclusions

The average sea ice thickness north of 70°N in CMIP3 models ranges from less than 1 m to more than 3 m in the late 20th century. The rate of sea ice thinning in the 21st century in these models is a strong function of the late 20th century thickness, such that models with above average thickness also thin faster than average. The average ice thickness north of 70°N across the CMIP3 models is highly correlated with the September ice extent, and therefore strongly influences marine ecosystems and early winter surface temperatures. Because sea ice thickness change depends sensitively on the mean state, error in a model's climatology gives rise to error in future predictions of ice thinning and extent.

I have shown that uncertainty in the strength of ice albedo feedback is probably not a major source of uncertainty for ice thinnning in future predictions. This result stems from the fact that the ice-albedo feedback factor on ice thickness f is rather small. I estimated f in a global climate model by holding the surface albedo of sea ice and ocean fixed while doubling CO_2. Ice-albedo feedback causes sea ice to thin about 26% more compared to a model run without ice-albedo feedback. A gain of 26% corresponds to a feedback factor of only $f = 0.21 \pm 0.02$, where the error here is an estimate of uncertainty in this one model (which is bound to be much smaller than the range of f across models).

Such a small value for f can only give rise to a fairly narrow estimate for thickness change provided the range of f across models is the sole source of uncertainty. Even if the uncertainty of f across models is as high as 100% (ranging from 0 to 0.42), it causes little uncertainty in the ice thickness change.

Instead the uncertainty in the mean state has a much larger influence on uncertainty in the thickness change. I have argued that the principal cause is the growth-thickness feedback, which is regulated by the conduction of heat through the ice. This feedback controls the adjustment to equilibrium and is strongly thickness dependent. Heat conduction depends roughly on the inverse of thickness, or $1/h$. When surface fluxes are perturbed, the ice thickness adjusts until the conduction of heat through the ice achieves surface energy balance. The thickness need not adjust very much for thin ice owing to the $1/h$ dependence. Consequently when the thickness is biased, the thickness change in response to a perturbation is also biased. A bias of ± 0.77 m, as from the CMIP3 models, gives rise to an uncertainty of more than ± 1 m for the thickness change due to doubling CO_2.

I have not explained why the models have so much spread in the mean state. Another paper in this monograph argues that a large portion of the error can be explained by the summertime atmospheric energy fluxes and the surface albedo in particular [*DeWeaver et al.*, 2008]. If this is the case, then modelers should do a better job reducing biases in the atmosphere and tuning the surface albedo to reduce the spread in model uncertainty for present and future prediction.

Acknowledgments. I am grateful for support from the National Science Foundation through grants ATM0304662 and OPP0454843. I thank Gerard Roe and Eric DeWeaver for helpful conversations and two anonymous reviewers whose comments greatly improved this paper. I thank the modeling groups, the Program for Climate Model Diagnosis and Intercomparison (PCMDI) and the WCRP's Working Group on Coupled Modelling (WGCM) for their roles in making available the WCRP CMIP3 multi-model dataset. Support of this dataset is provided by the Office of Science, U.S. Department of Energy.

References

Arzel, O., T. Fichefet, and H. Goosse, Sea ice evolution over the 20th and 21st centuries as simulated by the current AOGCMs, *Ocn. Mod.*, *12*, 401–415, 2006.

Bitz, C. M., and W. H. Lipscomb, An energy-conserving thermodynamic model of sea ice, *J. Geophys. Res.*, *104*, 15,669–15,677, 1999.

Bitz, C. M., and G. H. Roe, A mechanism for the high rate of sea-ice thinning in the arctic ocean, *J. Climate*, *18*, 3622–31, 2004.

Bitz, C. M., D. S. Battisti, R. E. Moritz, and J. A. Beesley, Low frequency variability in the arctic atmosphere, sea ice, and upper ocean system, *J. Climate*, *9*, 394–408, 1996.

Bitz, C. M., M. M. Holland, A. J. Weaver, and M. Eby, Simulating the ice-thickness distribution in a coupled climate model, *J. Geophys. Res.*, *106*, 2441–2464, 2001.

Bitz, C. M., J. K. Ridley, M. M. Holland, and H. Cattle, Global climate models and 20th and 21st century arctic climate change, in *Arctic Climate Change — The ACSYS Decade and Beyond*, edited by P. Lemke, p. accepted 2008.

Bony, S., et al., How well do we undersand and evaluate climate change feedback processes?, *J. Climate*, *19*, 3445–3482, doi:10.1175/JCLI3819.1, 2006.

Collins, W. D., et al., The Community Climate System Model, Version 3, *J. Climate*, *19*, 2122–2143, 2006.

Comiso, J. C., SSM/I concentrations using the Bootstrap Algorithm, *Tech. Rep. RP 1380, 40pp*, NASA, Technical Report, 1995.

DeWeaver, E., and C. M. Bitz, Atmospheric circulation and Arctic sea ice in CCSM3 at medium and high resolution, *J. Climate*, *19*, 2415–2436, 2006.

DeWeaver, E., E. C. Hunke, and M. M. Holland, Sensitivity of arctic sea ice thickness to inter-model variations in surface energy budget simulation, in *Arctic Sea Ice Decline: observations, projections, mechanisms, and implications*, edited by E. deWeaver, C. M. Bitz, and B. Tremblay, p. submitted, AGU, 2008.

Gregory, J. M., P. A. Stott, D. J. Cresswell, N. A. Rayner, and C. Gordon, Recent and future changes in Arctic sea ice simulate by the HadCM3 AOGCM, *Geophys. Res. Lett.*, p. 10.1029/2001GL014575, 2002.

Hibler, W. D., and J. K. Hutchings, Multiple equilibrium arctic ice cover states induced by ice mechanics, in *Ice in the Environment: Proceedings of the 16th IAHR International Symposium on Ice*, vol. Dunedin, New Zealand, Dec. 2002., pp. 228–237, 2002.

Hibler, W. D., J. K. Hutchings, and C. F. Ip, Sea ice arching and multiple flow states of arctic pack ice, *Annals of Glaciology*, *44*, 339–344, 2006.

Holland, M. M., and C. M. Bitz, Polar amplification of climate change in the Coupled Model Intercomparison Project, *Clim. Dyn.*, *21*, 221–232, 2003.

Holland, M. M., C. Bitz, and A. Weaver, The influence of sea ice physics on simulations of climate change, *J. Geophys. Res.*, *106*, 2441–2464, 2001.

Holland, M. M., C. M. Bitz, E. C. Hunke, W. H. Lipscomb, and J. L. Schramm, Influence of the sea ice thickness distribution on polar climate in CCSM3, *J. Climate*, *19*, 2398–2414, 2006a.

Holland, M. M., C. M. Bitz, and B. Tremblay, Future abrupt reductions in the summer arctic sea ice,, *Geophys. Res. Lett.*, *33, L23503*, doi:10.1029/2006GL028,024, 2006b.

Hunke, E. C., and J. K. Dukowicz, The elastic-viscous-plastic sea ice dynamics model in general orthogonal curvilinear coordinates on a sphere – incorporation of metric terms, *Mon. Wea. Rev.*, *130*, 1848–1865, 2002.

Lipscomb, W. H., Remapping the thickness distribution in sea ice models, *J. Geophys. Res.*, *106*, 13,989–14,000, 2001.

Meehl, G. A., et al., Climate change projections for the twenty-first century and climate change commitment in the CCSM3, *J. Clim.*, *19*, 2598–2616, 2006.

Roe, G. H., and M. B. Baker, Why is climate sensitivity so unpredictable?, *Science*, *218, doi:10.1126/science.1144735*, 629–632, 2007.

Springer, M. D., *The Algebra of Random Variables*, 470 pp., John Wiley & Sons, 1979.

Stroeve, J., M. M. Holland, W. Meier, T. Scambos, and M. Serreze, Arctic sea ice decline: Faster than forecast, *Geophys. Res. Lett.*, *34*, doi:10.1029/2007GL029,703, 2007.

Thorndike, A. S., A toy model linking atmospheric thermal radiation and sea ice growth, *J. Geophys. Res.*, *97*, 9401–9410, 1992.

Untersteiner, N., On the mass and heat budget of arctic sea ice, *Arch. Meteorol. Geophys. Bioklimatol., A*, *12*, 151–182, 1961.

Untersteiner, N., Calculations of temperature regime and heat budget of sea ice in the Central Arctic, *J. Geophys. Res.*, *69*, 4755–4766, 1964.

Winton, M., Sea ice-albedo feedback and nonlinear arctic climate change, in *Arctic Sea Ice Decline: observations, projections, mechanisms, and implications*, edited by E. deWeaver, C. M. Bitz, and B. Tremblay, p. submitted, AGU, 2008.

Zhang, X., and J. E. Walsh, Toward a seasonally ice-covered Arctic Ocean: Scenarios from the IPCC AR4 model simulations, *J. Climate*, *19*, 1730–1747, 2006.

C. M. Bitz, Atmospheric Sciences, MS 351640, University of Washington, Seattle, WA 98195-1640, USA. (bitz@atmos.washington.edu)